IRS-1–Rad51 nuclear interaction sensitizes JCV T-antigen positive medullblastoma cells to genotoxic treatment

ARTICLE *in* INTERNATIONAL JOURNAL OF CANCER · AUGUST 2006

Impact Factor: 5.09 · DOI: 10.1002/ijc.21828 · Source: PubMed

9 AUTHORS, INCLUDING:

Mateusz Koptyra
The Children's Hospital of Philadelphia
20 PUBLICATIONS **744** CITATIONS
SEE PROFILE

Antonio Giordano
Università Politecnica delle Marche
439 PUBLICATIONS **10,490** CITATIONS
SEE PROFILE

Kamel Khalili
Temple University
258 PUBLICATIONS **6,570** CITATIONS
SEE PROFILE

Krzysztof Reiss
Louisiana State University Health Sciences …
159 PUBLICATIONS **6,152** CITATIONS
SEE PROFILE

Int. J. Cancer: **119,** 539–548 (2006)

IRS-1–Rad51 nuclear interaction sensitizes JCV T-antigen positive medulloblastoma cells to genotoxic treatment

Joanna Trojanek[1], Thu Ho[1], Sidney Croul[1], Jin Ying Wang[1], Janaki Chintapalli[1], Mateusz Koptyra[2], Antonio Giordano[3], Kamel Khalili[1] and Krzysztof Reiss[1]*

[1]*Center for Neurovirology, Department of Neuroscience, Temple University, Philadelphia, PA, USA*
[2]*Department of Microbiology, Temple University, Philadelphia, PA, USA*
[3]*Sbarro Institute for Cancer Research and Molecular Medicine, Temple University, Philadelphia, PA, USA*

The large T-antigen from human polyomavirus JC (JCV T-antigen) is suspected to play a role in malignant transformation. Previously, we reported that JCV T-antigen requires the presence of a functional insulin-like growth factor I receptor (IGF-IR) for transformation of fibroblasts and for survival of medulloblastoma cell lines; that IGF-IR is phosphorylated in medulloblastoma biopsies and that JCV T-antigen inhibits homologous recombination-directed DNA repair, causing accumulation of mutations. Here we are evaluating whether JCV T-antigen positive and negative mouse medulloblastoma cell lines, which significantly differ in their tumorigenic properties, are also different in their abilities to repair double strand breaks of DNA (DSBs). Our results show that despite much stronger tumorigenic potential, JCV T-antigen positive medulloblastoma cells are more sensitive to genotoxic agents (cisplatin and γ-irradiation). Subsequent analysis of DNA repair of DSBs indicated that homologous recombination-directed DNA repair (HRR) was selectively attenuated in JCV T-antigen positive medulloblastoma cells. JCV T-antigen did not affect HRR directly. In the presence of JCV T-antigen, insulin receptor substrate 1 (IRS-1) translocated to the nucleus where it co-localized with Rad51, possibly attenuating HRR.

Key words: IRS-1; JC virus T-antigen; Rad51; genomic instability; medulloblastoma

Medulloblastomas are malignant WHO grade IV cerebellar tumors of the childhood.[1] These tumors originate from the external granular layer of the cerebellum and have an inherent tendency to spread *via* cerebrospinal pathways.[2] Interestingly, multiple genetic aberrations have been associated with the development of these neoplasms. Among them, loss of chromosome p17 and gain of 17q is detected in 50% of medulloblastomas[3] while losses on chromosomes 10q, 11, and gains on chromosome 7 are detected in more than 40% of the examined cases.[4] Rearrangements of chromosome 1 resulting in trisomy 1q without loss of the p-arm and allelic losses on chromosome 9 are also detected.[3] Other major alterations found in medulloblastomas include amplifications of the c-Myc and N-Myc genes[5]; β-catenin mutations; APC point mutations[6]; elevated expression of neuronal transcription factors PAX5 and PAX6[7]; increased protein levels of the insulin-like growth factor I receptor (IGF-IR) and insulin receptor substrate 1 (IRS-1).[8–11] Of interest, PCR-based and immunohistochemical detection of the JC virus (JCV) genome and viral proteins, including JCV T-antigen, has raised questions about the contribution of this common polyomavirus to the development of medulloblastoma.[12–15]

The genomic alterations and possible viral contribution suggest that mechanisms responsible for the maintenance of genomic integrity could be compromised in medulloblastomas. One feasible connection to the development of genomic instability is JCV T-antigen. Although its role in the etiology of human tumors is still controversial, JCV T-antigen readily transforms cells in culture and is tumorigenic in experimental animals.[8,14,16–18] In addition to the well-established effects of SV40, BKV and JCV T-antigens in deregulating the cell cycle,[19] these viral proteins are suspected to play a role in the development of genomic instability. Several studies have shown random chromosomal aberrations emerging at each consecutive passage of T-antigen positive cells.[20–24] The diversity of karyotypes found in cells carrying T-antigen implies that it causes random damage to the genome. One mechanism, which could explain this accumulation of random mutations, is a disturbance in repair of double strand breaks DNA (DSBs). DSBs, which can be lethal to the cell, arise from ionizing radiation, a variety of genotoxic chemicals and when replication forks encounter other DNA lesions such as cisplatin induced intra-strand cross-links.[25,26] To support cell survival, DSBs must be repaired by at least 1 of the 2 major DNA repair mechanisms: error free homologous recombination-directed DNA repair (HRR) or error prone non-homologous end joining (NHEJ).[25]

In the series of experiments reported in this article, we demonstrate that JCV T-antigen sensitizes murine medulloblastoma cells to genotoxic treatments including γ-irradiation and cisplatin. This is quite relevant since cisplatin is frequently used in the treatment of medulloblastoma patients.[27–30] Detailed analysis of the DNA repair of DSBs indicates that homologous recombination-directed DNA repair (HRR) is significantly impaired while NHEJ is practically unaffected in JCV T-antigen expressing murine medulloblastoma cell lines. Although we are unable to detect any direct interaction between JCV T-antigen and DNA repair proteins, we find IRS-1 at the sites of damaged DNA. Further analyses demonstrate that nuclear IRS-1 co-localizes with Rad51 and interferes with HRR when JCV T-antigen positive medulloblastoma cells attempt to repair cisplatin-induced DNA damage. These findings suggest that cooperative JCV T-antigen–IRS-1 inhibition of HRR may sensitize medulloblastoma cell lines to DNA damaging agents, suggest the mechanism by which JCV T-antigen could trigger genomic instability, and point to a T-antigen contribution to the development of malignancy in this cell type.

Material and methods

Cell lines

Mouse medulloblastoma cell lines, BsB8 and Bs-1a, derived from cerebellar medulloblastomas that developed spontaneously in transgenic mice expressing an early genome of the archetype form of the JC virus.[14] In addition, Bs-1a cells are JCV T-antigen negative, and BsB8 are JCV T-antigen positive.[11] Cells were cultured in Dulbecco's Modified Eagle Medium (DMEM) (GIBCO-BRL, Grand Island, NY) containing 10% fetal bovine serum (FBS), at 37°C in a 9.6% CO_2 atmosphere. The cells were further modified by a stable transfection with pDR-GFP (green fluorescent protein) reporter plasmid.[31] All cells were routinely cultured

Abbreviations: CNS: central nervous system; DSBs: DNA double strand breaks; GFP: green fluorescent protein; HRR: homologous recombination DNA repair; IRS-1: insulin receptor substrate 1; JCV: human polyomavirus JC; NHEJ: non-homologous end joining.

Grant sponsor: NIH; Grant numbers: RO1CA095518-01, PO1 NS36466-06.

***Correspondence to:** Center for Neurovirology, Department of Neuroscience, Biology Life Sciences Bldg. Room 230, School of Medicine, Temple University, 1900 North 12th Street, Philadelphia, PA 19122, USA. Fax: +215-204-0679. E-mail: kreiss@temple.edu

Received 19 September 2005; Accepted 15 December 2005
DOI 10.1002/ijc.21828
Published online 29 March 2006 in Wiley InterScience (www.interscience.wiley.com).

in DMEM supplemented with penicillin, streptomycin and 10% FBS. For the selection of stable DRGFP clones, culture media were supplemented with puromycin (2 μg/ml). In some experiments, quiescent cells were stimulated with IGF-I (50 ng/ml; GIBCO-BRL, Grand Island, NY).

Cell cycle analysis

Aliquots of cells, 1×10^6/ml, were fixed in 70% ethanol for 30 min at 4°C, cells were centrifuged at 1,600 rpm and the resulting pellets were resuspended in 1 ml of freshly prepared Propidium Iodide/RNaseA solution. Cell cycle distribution was analyzed by FACSCalibur (Becton-Dickinson, Franklin Lakes, NJ) using the CellQuest Program.[32]

Clonogenic assay

Cells were plated at 5×10^2 on 12-well culture plates (Costar, Corning, NY) in DMEM supplemented with 10% FBS. Following attachment, cells were treated with cisplatin at 0, 0.2, 0.5 and 1.0 μg/ml. In a separate set of experiments, cells were irradiated with 0, 5, 10 and 20 Gray (Gy) by utilizing the J.L Shepherd Mark I, Model 30-1 γ-irradiator. During irradiation, which lasted from 1.3 min (5 Gy) to 5.2 min (20 Gy), cells were kept at room temperature, and immediately after, cells were transferred on ice. Colonogenic potential was evaluated at day 14 after plating by staining the cells with 0.25% Brilliant Blue in methanol and macroscopic counting of clones.

Comet assay

Cells were either irradiated with 20 Gy of γ-irradiation, or treated with cisplatin (3 μg/ml). The DNA damage was analyzed by alkaline single cell gel electrophoresis (comet assay), as previously described,[33] with some modifications. Briefly, an aliquot of 1×10^5 cells was suspended in 0.75% low melting point agarose and spread on microscopic slides pre-coated with 0.5% NMP agarose (Sigma). The cells were lysed for 1 hr at 4°C in a buffer containing 2.5 M NaCl, 100 mM EDTA, 1% Triton X-100, 10 mM Tris, pH 10. The slides were placed in an electrophoresis unit and DNA was allowed to unwind for 40 min in the running buffer (300 mM NaOH, 1 mM EDTA, pH $>$ 13). Electrophoresis was conducted for 30 min at 0.73 V/cm. The slides were neutralized with 0.4 M Tris, pH 7.5, stained with 2 mg/ml 4′ 6′ diamedino-2-phenylindole and covered with cover slips. One hundred images were randomly selected from each sample, and the Olive tail moment was calculated using an image analysis system, the Comet 5.0 (Kinetic Imaging, Liverpool, UK).

Southern blot

This methodology was utilized to screen for integrated DRGFP cDNA and to estimate DRGFP copy number in the selected clones. Stable BsB8 and Bs-1a cell lines expressing the DRGFP reporter cassette were generated by Nucleofection of 1×10^6 cells with 2 μg of plasmid DNA in Solution T, according to Amaxa recommendations. Genomic DNA samples were obtained using DNeasy Tissue kit 250 (Qiagen Cat No 69506). Ten micrograms genomic DNA samples were digested using SalI and HindIII restriction enzymes (Promega), and were submitted to 0.8% agarose electrophoresis. Southern blots were carried out according to previously described methodology.[34] The 724 bp GFP probe was obtained from the pDR-GFP by NcoI/NotI digestion.

Homologous recombination directed DNA repair

The plasmid pDR-GFP (generously provided by Dr. M. Jasin, Sloan-Kettering Cancer Center, New York) was stably introduced, by calcium phosphate reagent (Promega, Madison WI), into BsB8 and Bs-1a medulloblastoma cell lines. Stable clones were selected in puromycin (2 μg/ml) and characterized by Southern blot. The pDRGFP contains a non-active gene for GFP (SceGFP) as a recombination reporter, and a fragment of the GFP gene as a donor for homologous repair.[31] The SceGFP cassette has an inactivating insertion, which consists of 2 STOP codons and a restriction site for the rare cutting endonuclease, I-*Sce*I. When I-*Sce*I is expressed in DR-GFP expressing clones, it inflicts DSBs within the SceGFP fragment providing a signal for homologous recombination and the reconstruction of functional GFP. To analyze the effectiveness of HRR, cells were transiently transfected with 3 μg of pCβA-Sce and 1 μg of pDsRed1-Mito (Clontech, Palo Alto, CA) utilizing Fugine 6 reagent (Roche, Indianapolis, IN). pCβA-Sce contains I-*Sce*I cDNA to generate DSBs in SceGFP cDNA[31] and pDsRed1-Mito contains red fluorescent protein with a mitochondrial localization signal to control for the efficiency of transfection. DNA repair by HRR was evaluated by counting cells with both green nuclear fluorescence and red mitochondrial fluorescence *versus* all positively transfected cells (only red cells + red and green cells) at 96 hr after transfection. Cells showing green nuclear fluorescence only were sporadically detected; however these cells were not considered in the calculation.

Non-homologous end joining

The cell-free NHEJ assay was followed,[35] and nuclear lysates were prepared according to the protocol previously described.[32] Briefly, NHEJ reactions were performed in the following conditions: 50 μg of nuclear lysate; 1 mM ATP; 0.25 mM dNTPs; 25 mM Tris-Acetate (pH 7.5); 100 mM potassium acetate; 10 mM magnesium acetate and 1 mM DTT. After 5 min of pre-incubation at 37°C the reaction mixture was supplemented with the substrate (500 ng of XhoI–XbaI linearized pBluescript KS+). The reaction was incubated for 1 hr at 37°C to ligate the plasmid and treated with proteinase K to digest DNA bound proteins. Products of NHEJ reaction were resolved in 0.6% agarose gel containing 0.5 μg/ml of ethidium bromide.

Western blot and immunoprecipitation

To evaluate levels of the selected DNA repair proteins, monolayer cultures were lysed for 5 min on ice with 400 μl of lysis buffer A [50 mM HEPES; pH 7.5; 150 mM NaCl; 1.5 mM $MgCl_2$; 1 mM EGTA; 10% glycerol; 1% Triton X-100; 1 mM phenylmethylsulfonyl fluoride (PMSF); 0.2 mM Na-orthovanadate and 10 μg/ml aprotinin]. To improve recovery of DNA bound proteins, DNAse was added to the lysis buffer. Total proteins (50 μg) were separated on a 4–15% gradient SDS-PAGE (BioRad). The resulting blots were probed with following rabbit polyclonal antibodies: anti-Rad51 (Ab-1, Oncogene), anti-Rad52 (H-300; Santa Cruz), anti-Rad54 (H-152 Santa Cruz), anti-Ku70 (Serotec, UK) and anti-Ku80 (Serotec, UK). Anti-Grb-2 antibody (Transduction Laboratories, Lexington, KY) was used to monitor equal loading conditions.[32] A cell fractionation procedure was applied to separate cytoplasmic and nuclear proteins using the Nuclear/Cytosol Fractionation kit (BioViosion, Mountain View, CA) with some modifications. Rad51 was immunoprecipitated from 500 μg of nuclear or cytosolic extracts with anti-Rad51 mouse monoclonal antibody (clone 3C10; UBI) and agarose conjugated anti-mouse antibody (Sigma, St. Louis, MO). Corresponding blots were developed first with anti-IRS-1 rabbit polyclonal antibody (UBI, Lake Placid, NY), and were re-probed with anti-SV40 T-antigen mouse monoclonal antibody (Oncogene/Calbiochem, San Diego, CA), which detects JCV T-antigen,[36] and with anti-Rad51 mouse monoclonal antibody. To evaluate purity of nuclear and cytosolic fractions, anti-c-Jun mouse monoclonal antibody (KM-1, Santa Cruz) and anti-GAPDH mouse monoclonal antibody (RDI) were utilized, respectively. Finally, to evaluate phosphorylation status of nuclear and cytosolic IRS-1, anti-pY612 IRS-1 and anti-pS616 IRS-1 rabbit polyclonal antibodies were utilized (BioSource, Camarillo, CA).

Immunocytofluorescence

All cells were cultured on poly D-lysine coated Lab-Tek Chamber Slides (Nalge Nunc International, Rochester, NY). Cisplatin treatment, 1 μg/ml, was applied to exponentially growing cells for a period of 6 hr. For immunostaining, cells were fixed and permeablized with the buffer containing 0.02% Triton X-100 and 4%

formaldehyde in PBS. Fixed cells were washed twice in PBS and blocked in 1% BSA for 1 hr at 37°C. RAD51 was detected by mouse anti-RAD51 monoclonal antibody (UBI, Lake Placid, NY) followed by FITC-conjugated goat anti-mouse secondary antibody (Molecular Probes, Inc. Eugene, OR). IRS-1 was detected with rabbit anti-IRS-1 antibody (UBI, Lake Placid, NY), which recognizes the C-terminal portion of the IRS-1 protein, and rhodamine-conjugated goat anti-rabbit secondary antibody (Molecular Probes). Finally, phospho-histone H2AX was detected by a mouse monoclonal antibody, which recognizes phosphorylated serine within the 134–142 aa fragment of human histone H2AX (UBI, Lake Placid, NY), and rhodamine-conjugated goat anti-mouse secondary antibody (Molecular Probes). Negative controls were routinely performed in the presence of irrelevant, anti-BrdU antibody instead of primary antibodies. The images were visualized with an inverted Olympus 1 × 70 fluorescence microscope equipped with a Cook Sensicom ER camera (Olympus America, Melville, NY). In some cases, a series of 3D images of each individual picture were deconvoluted to 1 2D picture and resolved by adjusting the signal cut-off to near maximal intensity to increase resolution. Final pictures were prepared with Adobe Photoshop to demonstrate subcellular localization and co-localization between detected proteins.

Results

JCV T-antigen sensitizes medulloblastoma cells to DNA damage

Two previously characterized mouse medulloblastoma cell lines, BsB8 and Bs-1a, were used in this study.[11,37] Both derive from cerebellar tumors, which develop spontaneously in transgenic mice expressing JC virus early genome under the control of its archetype regulatory region.[14] Interestingly, the cells forming cerebellar tumors have a tendency of losing JCV T-antigen. This has allowed the selection of JCV T-antigen positive (BsB8) and JCV T-antigen negative (Bs-1a) medulloblastoma cell lines.[11,38] Results in Figures 1*a* and 1*b* demonstrate that the treatment with cisplatin is much more effective when applied to cells, which express JCV T-antigen (BsB8). The percentage of apoptosis, determined by TUNEL assay, increased dramatically in proliferating cultures of BsB8 cells (10% FBS) following a 24-hr treatment with cisplatin applied at indicated concentrations (Panel *a*). JCV T-antigen negative Bs-1a cells were much more resistant, showing 4-fold and 3.4-fold less apoptosis at 1 and 3 μg/ml of cisplatin, respectively (panel *a*). Elevated sensitivity to cisplatin was also demonstrated by clonogenic assay (panel *b*). A striking difference in clonogenic potential between BsB8 and Bs-1a medulloblastoma cells was observed at 0.75 μg/ml of cisplatin. At that concentration, BsB8 cells were practically unable to form clones while Bs-1a cells were only slightly affected. Although at higher concentrations of the drug both cell lines were severely affected, Bs-1a cells were still able to form an average of 20 clones after 1 μg/ml of cisplatin treatment. At this concentration, BsB8 cells were completely inhibited. One possible explanation for this enhanced sensitivity to cisplatin in the presence of JCV T-antigen could be an elevated rate of cell proliferation. This is because DNA cross-links, which are initially formed in the presence of cisplatin, can progress to lethal DSBs when replication forks stall at these primary DNA lesions. Flow cytometric measurements however indicated a similar cell cycle distribution pattern between BsB8 and Bs-1a cells. Unsynchronized monolayer cultures of BsB8 and Bs-1a cells were characterized by 43.8% ± 0.8 and 45.2% ± 0.3 cells in G1 phase; 23.2% ± 0.1 and 21.1% ± 1.4 cells in S phase; 32.4% ± 0.9 and 33.4% ± 1.2 cells in G2/M phase, respectively. Since cell cycle distribution was similar in both cell lines, we asked whether the presence of JCV T-antigen affects the level of DNA damage and overall DNA repair following 2 genotoxic treatments, cisplatin and γ-irradiation. To evaluate these parameters, we employed single cell electrophoresis (comet assay). Note however, that comet evaluation of cellular DNA is less sensitive for cisplatin than for γ-irradiation induced damage. This is because intra-strand cross-links formed after cisplatin treatment partially prevent the development of typical comets despite of the fact that single and double strand breaks are also present.[39] With this in mind, we performed separate assays for γ-irradiation and for cisplatin-induced DNA damage (Fig. 1*d*). The results in Figure 1*c* show that both cell lines have a similar initial rate of DNA damage after receiving 20 Grays (Gy) of γ-irradiation (compare values determined at ''0 min'' time point). Similarly, we did not observe any major differences between BsB8 and Bs-1a cells when DNA damage was inflicted by cisplatin (Fig. 1*d*). Note, however, that in the presence of cisplatin values of Olive tail moments are expectedly lower, and DNA breaks appear much later in comparison to γ-irradiation induced DNA damage.[39] Further evaluation of the data in Figures 1*c* and 1*d* indicates that not only are the initial levels of DNA damage similar between BsB8 and Bs-1a cells, but the overall DNA repair seems to be unaffected by the presence of JCV T-antigen (compare ''5 min'' and ''15 min'' time points from γ-irradiation; 24 and 48 hr time points from cisplatin). This was quite unexpected considering that BsB8 cells are much more sensitive to cisplatin than Bs-1a cells (Figs. 1*a* and 1*b*). Although the overall levels of DNA repair evaluated by the comet assay are similar, the sensitivity of this methodology may not be sufficient to detect changes at the level of specific DSBs repair mechanisms such as homologous recombination-directed DNA repair (HRR) or non-homologous end joining (NHEJ).

DNA repair of double strand breaks

Since JCV T-antigen has been detected in some medulloblastoma biopsies,[13,40] and its presence sensitizes medulloblastoma cell lines to genotoxic treatments (Fig. 1), we asked whether JCV T-antigen affects molecular mechanisms responsible for DNA repair of DSBs. We first generated and characterized clones of BsB8 and Bs-1a cells, which stably express a GFP-based reporter system to evaluate HRR. Figure 2*a* illustrates Southern blot analysis of Sal I/Hind III digested genomic DNA demonstrating an intact DRGFP cassette in 2 BsB8 and 2 Bs-1a clones. Note that 3021 bp and 812 bp bands are detectable in positive control (TK-DRGFP), and in selected DRGFP medulloblastoma cell lines. Next, 2 clones BsB8/DRGFP#10 and Bs-1a/DRGFP#2, which exhibit the same digestion pattern and similar band intensities were electroporated with I-Sce-1 and mito-red expression vectors and were allowed to repair I-Sce-1-inflicted DNA breaks for an additional 4 days (see Methods). The results depicted in Figure 2*b* clearly indicate that among positively transfected cells (red fluorescence), the percentage of cells that repaired the damaged DRGFP cassette and reconstituted green nuclear fluorescence was 3-fold higher ($n = 3$) in Bs-1a/DRGFP#2 than in BsB8/DRGFP#10 cells. The same attenuation of HRR was observed with other 2 clones and in several experiments in which parental BsB8 and Bs-1a cells were transiently transfected with the DRGFP cassette (not shown). Additional support for this observation is provided by experiments in mouse embryo fibroblasts in which T-antigen also inhibited HRR.[41]

NHEJ, the second DSBs repair mechanism, is considered a quick and effective way to ligate DSBs, which may well introduce mutations. We have used a cell-free assay to evaluate NHEJ. The results in Figure 3*a* illustrate the formation of multiple bands from the linear plasmid DNA as a result of NHEJ. A slight reduction in the efficiency of NHEJ was observed in the presence of nuclear extracts from BsB8 in comparison to Bs-1a cells. Densitometric analysis (Panel *b*) was performed for the linear plasmid, dimers, trimers and tetramers, respectively. Although the differences were not significant, lower intensities of the linear plasmid (substrate) and slightly elevated densities of the corresponding multimers (products) were consistently observed in nuclear extracts from Bs-1a in comparison to BsB8 cells ($n = 2$).

DNA repair protein levels and sub-cellular localization

In view of the strong inhibition of HRR in the presence of JCV T-antigen, we evaluated levels and subcellular localization of several major DNA repair proteins. As shown in Figure 4*a*, levels of the selected HRR proteins including Rad51, Rad52 and Rad54 were comparable in proliferating unsynchronized cultures of Bs-

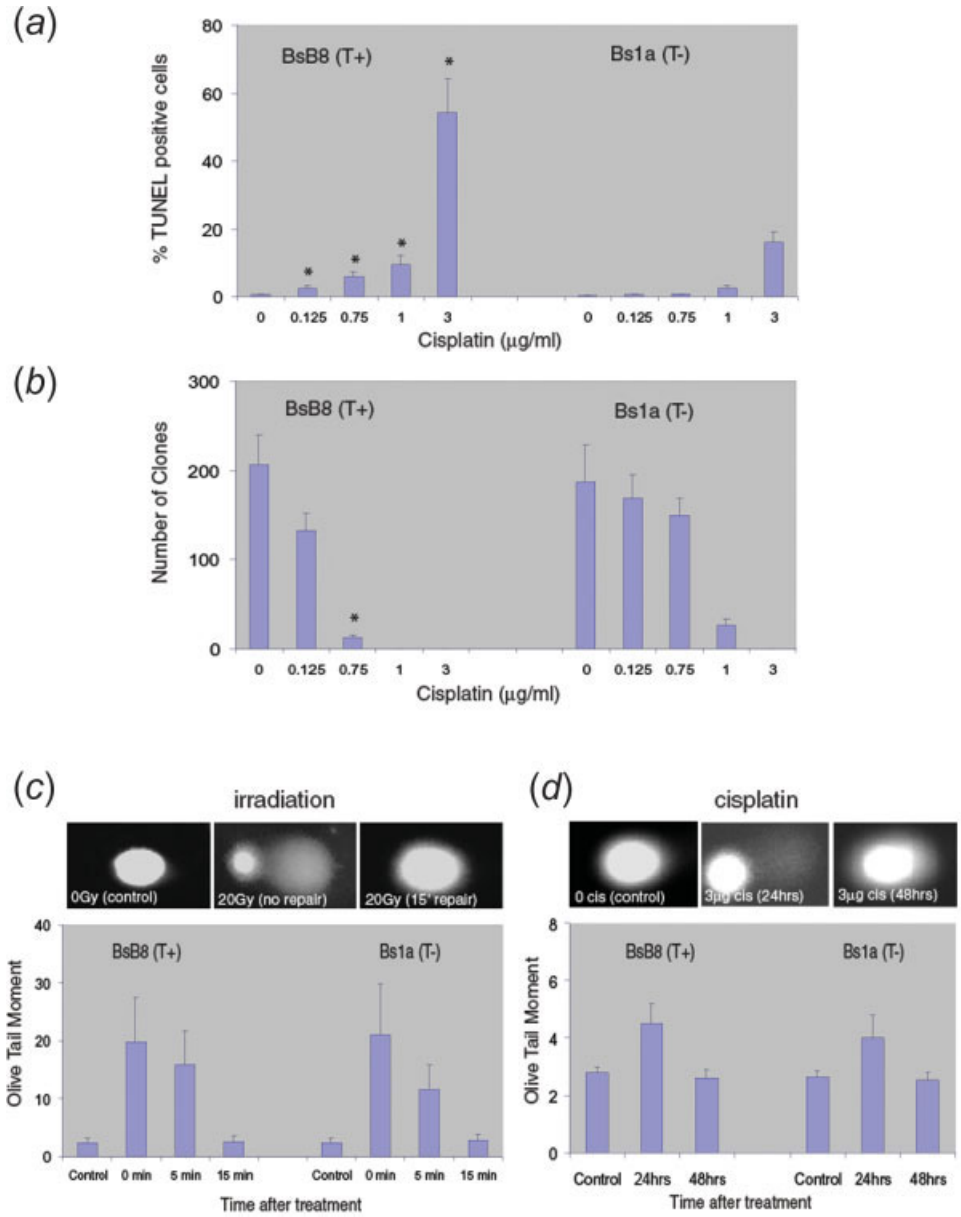

FIGURE 1 – JCV T-antigen inhibits cell growth and cell survival after DNA damage. JCV T-antigen positive (BsB8; T+) and negative (Bs1a; T−) mouse medulloblastoma cell lines were treated with indicated concentrations of cisplatin (*a*, *b* and *d*), or with 20 Gy of γ-irradiation (*c*). To evaluate the extent of cell death by apoptosis (*a*), TdT reaction (TUNEL assay) was applied to cell cultures growing in the presence of 10% FBS and cisplatin (cisplatin concentration ranging from 0 to 3 μg/ml) for 24 hr. Data represent an average of 3 experiments with standard deviation. * indicates values that are significantly different between BsB8 and Bs-1a at corresponding cisplatin concentrations. Note an apparent increase of apoptosis in BsB8 cells observed at 1 and 3 μg/ml of cisplatin. (*b*) Clonogenic growth of BsB8 and Bs-1a was evaluated following the treatment with indicated concentrations of cisplatin. Following 24 hr incubation with cisplatin, the cells were plated at clonal density (1×10^3/35-mm dish) and the number of clones was determined at day 14 after plating. Data represent an average of 2 experiments. * indicates values that are significantly different between Bs-1a and BsB8 at corresponding concentrations of cisplatin. (*c* and *d*) DNA damage and DNA repair evaluated by single cell electrophoresis (comet assay). The assay was performed either after cell exposure to 20 Gy of γ-irradiation (*c*), or cisplatin treatment (*d*). After irradiation, BsB8 and Bs1a cells were either placed on ice (0 min maximal damage), or were incubated for 5, and 15 min at 37°C (time of DNA repair). Cells were subjected to single cell electrophoresis and stained with propidium iodide. Control cells were left without irradiation. For the cisplatin treatment, DNA damage was evaluated in exponentially growing cultures after 24 and 48 hr incubation with cisplatin (3 μg/ml). Data represent an average of Olive tail moment with standard deviation and were calculated by Comet 6 software based on 3 experiments in which 100 cells per experiment were measured. Insets: Representative images of DNA damage observed in BsB8 cells after single cell electrophoresis following γ-irradiation (*c*) and cisplatin treatment (*d*).

1a and BsB8 cells. Similarly, levels of NHEJ proteins, KU70, KU80 and DNA PK, were also not affected by the presence of JCV T-antigen.

Since DNA repair proteins form multi-protein complexes at the sites of damaged DNA (nuclear foci), we employed immunocytochemical detection to determine whether JCV T-antigen co-localizes with these DNA/protein complexes possibly affecting their function. Following the induction of DSBs by cisplatin, immunolabeling with anti-Rad51 antibody revealed a large number of nuclear foci in Bs-1a and BsB8 cells (Fig. 4*b*). In the same micro-

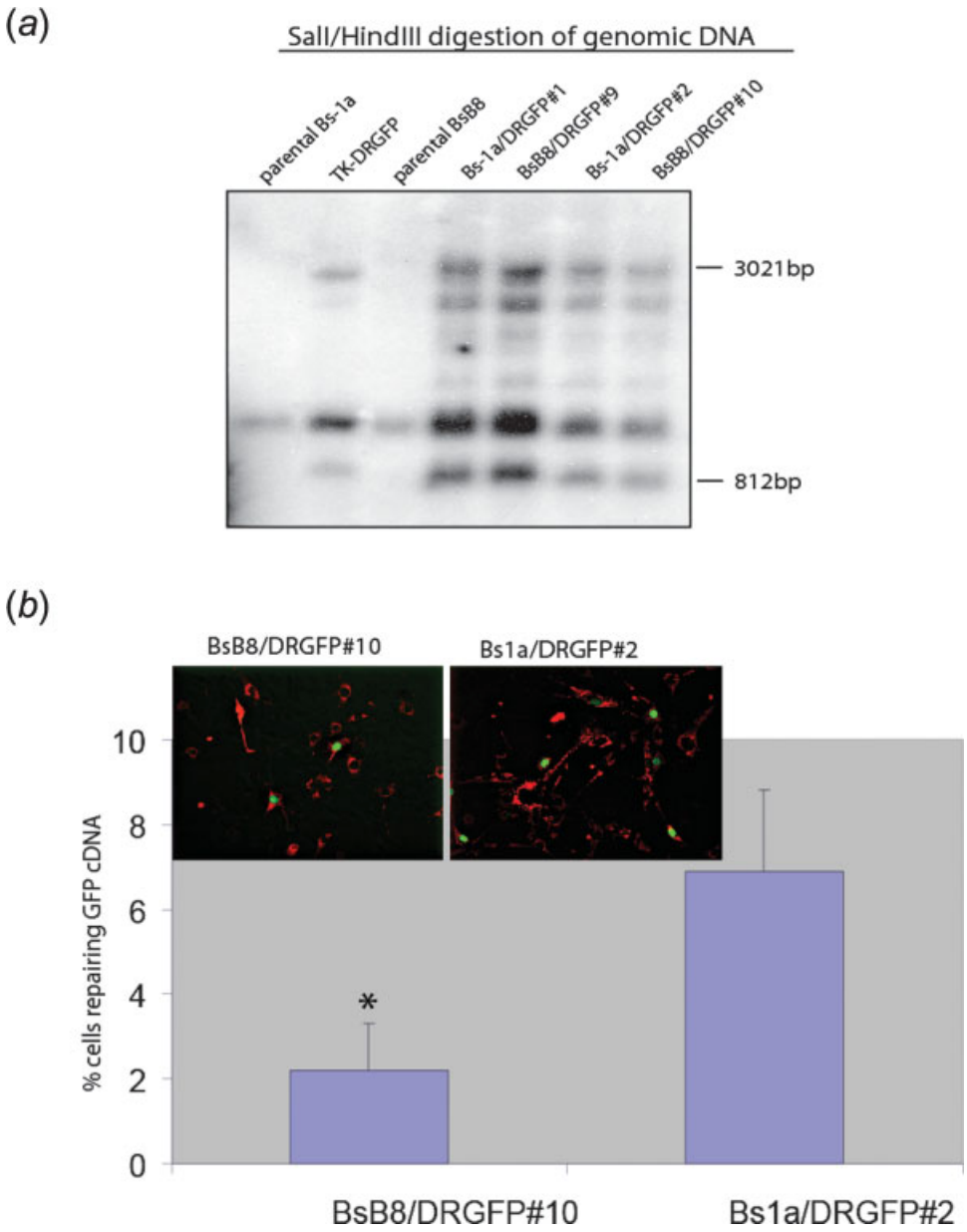

FIGURE 2 – JCV T-antigen affects DNA repair of double strand breaks (DSBs). (*a*) Southern blot analysis to detect an intact DRGFP reporter cassette in BsB8 and Bs-1a medulloblastoma cell lines. Genomic DNA was isolated from the parental BsB8 and Bs-1a cells (negative controls), from Tk⁻DRGFP cells[41] (positive control), and from several clones of Bs-1a and BsB8 stably transfected with the DRGFP reporter cassette. SalI/HindIII–digestion released expected 3021 bp and 812 bp GFP fragments from the DRGFP positive cell lines. (*b*) Homologous recombination directed DNA repair (HRR) was evaluated by the assay based on the reconstruction of the wild type green fluorescent protein (GFP) from 2 non-functional heteroallelic fragments of GFP cDNA delivered into cells by the pDRGFP expression vector. HRR was evaluated in BsB8/DRGFP (clone #10) and Bs-1a/DRGFP (clone #2) following transient transfection with the expression vector for I-*Sce-I* rare cutting endonuclease, to inflict DNA double strand break in GFP cDNA, and with mito- red containing expression vector, to control for the efficiency of transfection. The results were collected from 3 separate experiments, in duplicate ($n = 6$) in which about 2000 positively transfected cells/experiment were counted in at least 10 randomly selected microscopic fields. * indicates statistical significance ($p < 0.05$). Inset: fluorescent images taken at day 4 following the I-*Sce-I* and mito-red transfection. Note the presence of cells with an apparent green nuclear fluorescence following HRR-mediated reconstitution of GFP function.

scopic fields, anti-T-antigen antibody labeled BsB8 nuclei intensely and the immunolabeling was negative in Bs-1a cells. Superimposition of the Rad51 (green) and T-antigen (red) images revealed very restricted co-localization between these 2 proteins even in BsB8 cells. Quantitatively, 7.35% ± 1.8 of total Rad51 co-localized with JCV T-antigen (evaluated by SlideBook4 deconvolution software and appropriate mask operation, according to manufacturer recommendations; Intelligent Imaging Innovations, Denver). Although this implies that only a small fraction of these 2 proteins interact with each other, it does not exclude binding of JCV T-antigen to the regions of chromatin adjacent to DSBs. To investigate this possibility, BsB8 cells were immunolabeled with antibodies against T-antigen and phosphorylated histone H2AX (γH2AX). This immunolabeling was performed because histone H2AX is phosphorylated within mega bp regions surrounding DNA strand breaks.[42] Despite strong immunolabeling obtained for both γH2AX and JCV T-antigen, the overlapped images again demonstrated only sporadic yellow foci in which JCV T-antigen and γH2AX co-localized (arrows). Quantitatively, 8.85% ± 0.8 of total γH2AX co-localized with JCV T-antigen. In control reactions, in which JCV T-antigen negative Bs-1a cells were employed, the results of co-localization using anti T-antigen, Rad51 and γH2AX antibodies were obviously negative (Fig. 4*b* lower panel).

Nuclear interaction between IRS-1 and Rad51 in JCV T-antigen positive medulloblastoma cells

Based on our previous observation that IRS-1 interacts with Rad51, both in the perinuclear cytoplasm[32] and in the nucleus,[41] we asked whether IRS-1 participates in JCV T-antigen-mediated attenuation of HRR in the murine medulloblastomas. Following cisplatin treatment, BsB8 and Bs-1a cells were double immunolabeled with anti-Rad51 and anti-IRS-1. Figure 5*a* illustrates the abundant Rad51 nuclear foci detected in both Bs-1a and Bsb8 cell lines; cytoplasmic immunolabeling with anti-IRS-1 antibody detected in Bs-1a cells; and strong nuclear IRS-1 immuno-labeling detected in BsB8 cells. Superimposition of these images (overlap) shows an intensive co-localization between Rad51 and IRS-1 (yellow fluorescence). In the absence of JCV T-antigen, the only co-localization between Rad51 and IRS-1 was detected in the perinuclear cytoplasm of Bs-1a cells.

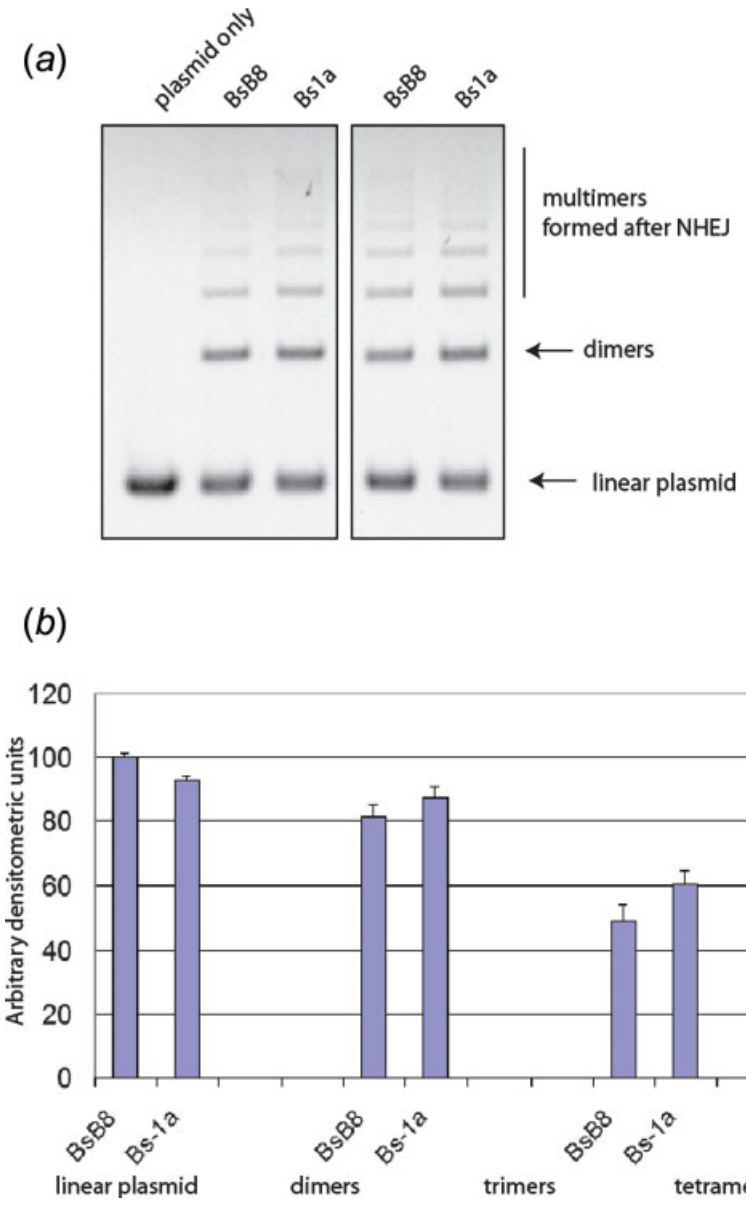

FIGURE 3 – Evaluation of NHEJ by a cell-free system. (*a*) Exponentially growing BsB8 and Bs-1a cells were compared. Corresponding nuclear extracts were utilized to ligate linear pBluscript KS+. The DNA bands are visualized on 0.6% agarose gel containing ethidium bromide. The control reaction represents linear plasmid DNA not treated with nuclear extracts. Arrows indicate positions of the linear plasmid (substrate), dimmers and subsequent multimers generated as a result of NHEJ. (*b*) Quantitative evaluation of the results from (*a*) by densitometric analysis with Scion software ($n = 2$). Comparisons between BsB8 and Bs-1a cells are shown for the linear plasmid, dimmers trimers and tetramers, respectively. Although differences are not significant, note consistently lower intensity of the linear plasmid (substrate) and higher densities for corresponding multimers (products) detected in Bs-1a in comparison to BsB8.

Subcellular fractionation, immunoprecipitation and Western blots were employed to confirm the nuclear interactions between Rad51 and IRS-1 (Fig. 5*b*). Following IRS-1 immunoprecipitation (IP), Rad51 was detected in both nuclear (N) and cytosolic (C) fractions of BsB8 cells. Similar results were obtained when Rad51 was immuno-precipitated and corresponding Western blot was developed with anti-IRS-1 antibody. In Bs-1a cells, however, the interaction between Rad51 and IRS-1 was detected predominantly in the cytosolic fraction. Blots from panel *b* were re-probed with anti-IRS-1 and anti-Rad51 antibodies to indicate amounts of these proteins after immuno-precipitations. In addition, purity of subcellular fractions isolated from BsB8 and Bs-1a cells, as well as the status of IRS-1 and JCV T-antigen are shown in Figure 5*c*. As expected, IRS-1 was abundant in both cytosolic and nuclear fraction of BsB8 cells and was present exclusively in the cytosolic fraction of Bs-1a cells.[36] JCV T-antigen was predominant in the nuclear fraction of BsB8 cells and was undetectable in both fractions isolated from Bs-1a cells. The blots were also probed with anti-c-jun and anti-GAPDH antibodies, which illustrated low levels of cross-contamination between the fractions.

Since previous results from our laboratory indicated that only hypo-phosphorylated IRS-1 was capable of binding Rad51,[32] we evaluated tyrosine phosphorylation of nuclear and cytosolic IRS-1 in JCV T-antigen positive BsB8 cells (Fig. 5*d*). The tyrosine phosphorylation of IRS-1 was detected exclusively in the cytosolic fractions of BsB8 cells, and the intensity of this band increased after IGF-I stimulation. In contrast, serine phosphorylated IRS-1 was prevalent in the nuclear fraction and the intensity of the band did not change following IGF-I stimulation. Since IRS-1 tyrosine phosphorylation inhibits cytosolic interaction between IRS-1 and Rad51,[32] and IRS-1 serine phosphorylation attenuates IRS-1–JCV T-antigen binding,[36] this could explain very low level of JCV T-antigen detected during DNA repair in IRS-1–Rad51 nuclear complexes (Fig. 4*b*).

In summary, we demonstrate that: (*i*) JCV T-antigen sensitizes medulloblastoma cells to genotoxic treatments; (*ii*) IRS-1 binds Rad51 at the multiple sites of damaged DNA in medulloblastoma cells expressing JCV T-antigen; (*iii*) nuclear IRS-1 detected in BsB8 cells is preferentially phosphorylated on serine residues; and

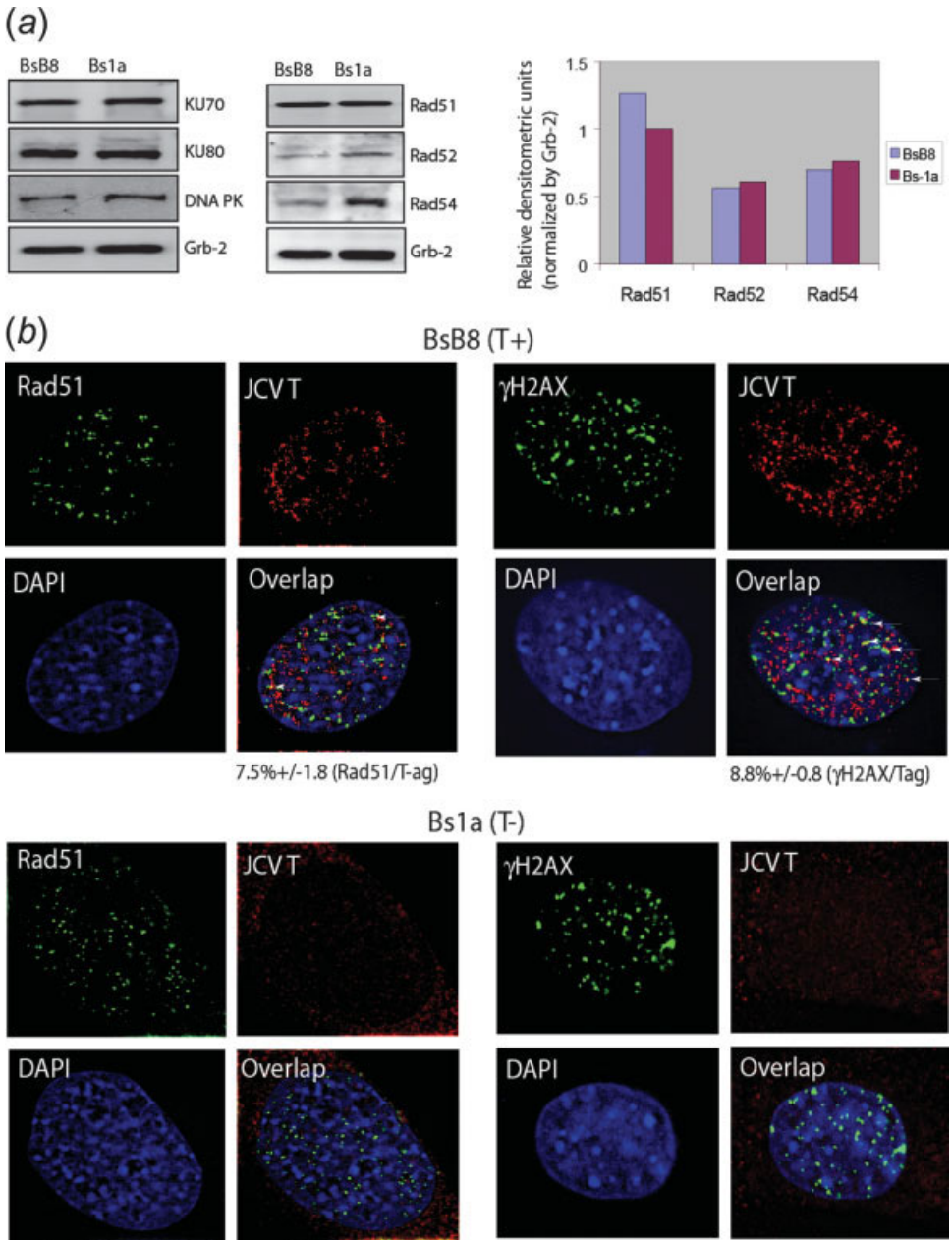

FIGURE 4 – Effects of JCV T-antigen on selected DNA repair proteins. (*a*) Protein extracts were isolated from exponentially growing BsB8 (JCV T-antigen positive; T+) and Bs-1a (JCV T-antigen negative; T−) cells. Total proteins (50 μg) were separated on PAGE and the resulting nitrocellulose filters were probed with antibodies against selected proteins involved in homologous recombination directed DNA repair (Rad51, Rad52 and Rad54) and non-homologous end joining (KU70, KU80 and DNA PK). The antibody against Grb-2 was utilized to monitor loading conditions. The histogram illustrates densitometry analysis of the HRR blot, and was normalized by Grb-2 protein level for each sample. (*b*) Subcellular localization of JCV T-antigen after DNA damage. Exponentially growing BsB8 and Bs-1a cells were treated with cisplatin (1 μg/ml) for 6 hr to inflict DSBs. Possible interactions between JCV T-antigen, Rad51 and phosphorylated histone H2AX (γH2AX) were examined by double immunolabeling of cells with anti-JCV T-antigen (red) and anti-Rad51 (green) antibodies, or with anti-JCV T-antigen (red) and anti-γH2AX (green) antibodies. Digital sectioning of images was performed by inverted fluorescent microscope equipped with motorized Z-axes and deconvolution software (SlideBook 4). Images marked ''overlap'' represent superimposition of 2 corresponding images shown in the same set of pictures, respectively. The numbers below overlap images indicate the percentage of colocalization between JCV T-antigen, Rad51 and γH2AX calculated from 3 separate images, considering the entire volume of corresponding nuclei.

(*iv*) phosphorylation state of the nuclear IRS-1 seems independent of IGF-I stimulation.

Discussion

It has been known for some time that DNA viruses are associated with a variety of types of human cancer.[19,43–45] In several studies, the human neurotropic polyomavirus JC (JCV) DNA has been detected in human brain tumors including medulloblastoma.[13,40,46,47] The oncogenic potential of this virus has been established in experimental animals. Intra-cerebral inoculation of JCV into owl and squirrel monkeys results in astrocytomas.[48,49] Intra-cerebral inoculation of newborn Golden Syrian hamsters with JCV has induced a broad range of tumors including medulloblastoma, astrocytoma and glioblastoma.[50,51] Injection of JCV into the brains of newborn rats causes undifferentiated neuroectodermal tumors in 75% of animals.[52] Among the viral proteins suspected to cause cellular transformation, the polyomavirus T-antigens have repeatedly been shown to transform cells *in vitro* and to induce tumor growth in experimental animals. Indeed, transgenic mice, which express early JCV genome coding for both small and large T-antigens, develop adrenal neuroblastomas,[53] and primitive neuroectodermal tumors.[14] Although the mechanism by which JCV T-antigen transforms cells remains to be elucidated, several molecular pathways have been implicated. These include well-documented binding and inactivation of the Rb family of nuclear proteins[54] and the binding between JCV T-antigen and p53.[38,55] In regards to genomic stability, recent studies have established that wt p53 plays an important role in restricting the magnitude of HRR at the level of stalled replication forks.[56] This new function of p53 in modulating DSBs DNA repair seems to be independent from other well known functions of p53 such as its role in cell cycle control and apoptosis, which are mediated through the p53 transcriptional activity,[57] and represent the major p53 function impaired by large T-antigens. This novel inhibition of HRR appears to operate through a direct interaction between serine phosphorylated p53 (pS15) and Rad51[58] and seem to prevent

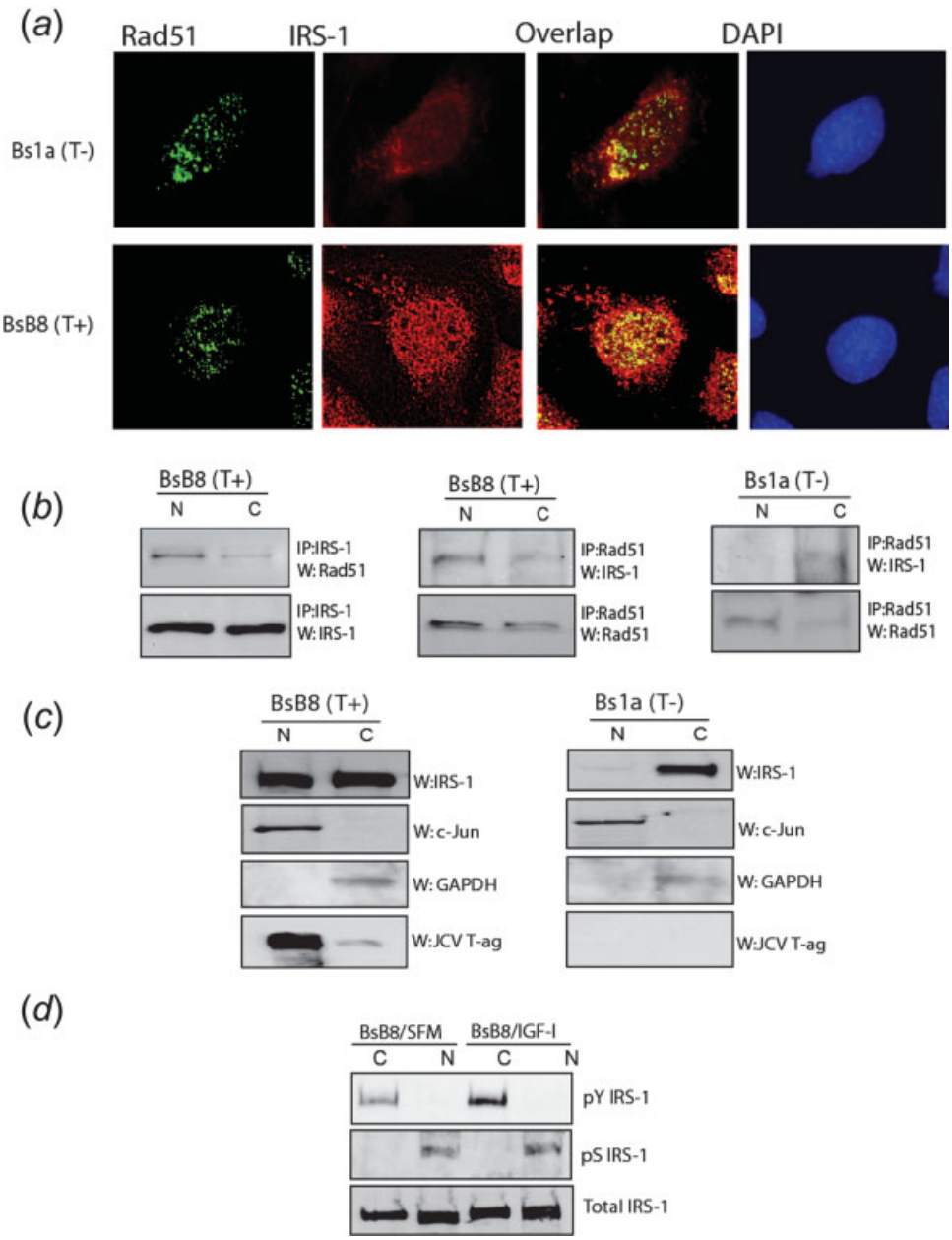

FIGURE 5 – IRS-1–Rad51 nuclear interactions. (*a*) Double immunolabeling with anti-Rad51 (green) and anti-IRS-1 (red) antibodies was applied to JCV T-antigen negative (Bs1a; T−) and positive (BsB8; T+) cells at 6 hr after the treatment with cisplatin (1 μg/ml). Images marked ''Overlap'' represent superimposition of 2 previous images depicted in the same row, respectively. Digital sectioning by deconvolution software indicates lack of nuclear co-localization between IRS-1 and Rad51 in T-antigen negative cells (Bs1a; T−). In contrast, JCV T-antigen positive cells (BsB8/T+) show nuclear co-localization between these 2 proteins (yellow fluorescence). (*b*) IP/Western analyses targeting Rad51–IRS-1 interaction. Experiments were performed either in cytosolic (C) or nuclear (N) fractions of BsB8 and Bs-1a medulloblastoma cell lines. Five hundred micro grams of protein lysates were immunoprecipitated (IP) either with anti-Rad51 or anti-IRS-1 antibodies and corresponding blots were developed with anti-Rad51 and anti-IRS-1 antibodies, or with anti-IRS-1 and anti-Rad51 antibodies, respectively. (*c*) Western blot analysis illustrating subcellular localization of IRS-1 and JCV T-antigen, and the purity of nuclear (N) and cytosolic (C) fractions. The blot was probed first with anti-IRS-1 antibody, and was re-probed with anti-c-Jun (for nuclear fraction), anti-GAPDH (for cytosolic fraction) and anti-T-antigen antibodies, respectively. (*d*) Western blot analysis showing phosphorylation status of IRS-1 detected in nuclear (N) or cytosolic (C) fractions from BsB8 cells in the presence (IGF) or absence (SFM) of IGF-I stimulation. The blot was probed first with anti-pY612 IRS-1 antibody, and was re-probed with anti-pS616 IRS-1 antibody, and anti-IRS-1 antibody, which recognizes total IRS-1 independently from its phosphorylation status (UBI).

excessive gene conversion, which itself can lead to genomic instability. The results presented in this paper demonstrate that JCV T-antigen sensitizes murine medulloblastoma cells to genotoxic agents (cisplatin, γ-irradiation). Analysis of DNA repair indicates that HRR is inhibited in JCV T-antigen positive medulloblastomas. This downregulation of HRR in the presence of JCV T-antigen is quite unexpected, since anticipated inactivation of p53 by JCV T-antigen should, at least in theory, release p53-mediated repression of HRR. One explanation could be that the binding between JCV T-antigen and p53 leaves at least one of the p53 domains (aa 264–315) free for the interaction with Rad51.[57] Therefore, it is reasonable to speculate that JCV T-antigen–p53 interaction does not eliminate p53-mediated inhibition of HRR.

The mechanism by which JCV T-antigen attenuates HRR seems to be indirect, as already proposed in our earlier study on mouse embryo fibroblasts.[41] The pathway involves JCV T-antigen interaction with IRS-1, which results in nuclear translocation of the IRS-1–JCV T-antigen complex. This finding is in agreement with several investigators who have postulated an interaction between polyomavirus large T-antigens and IRS-1.[36,59,60] In addition, our previous work and that of others has provided strong evidence for nuclear translocation of IRS-1 in the presence of SV40 and JCV T-antigens.[36,37,61,62] To date, the only defined nuclear function of IRS-1 has been nucleolar interaction between IRS-1 and the RNA polymerase I activator, UBF1.[63,64] Our results show that the IRS-1 fraction that translocates to the nucleus in the presence of JCV T-antigen co-localizes to the sites of damaged DNA where it interacts with Rad51. This clearly implicates IRS-1 in the process of HRR. Considering that NHEJ is practically unaffected by JCV T-antigen (Fig. 3), it also suggests that enhanced sensitivity to cisplatin observed in T-antigen positive cells may be due to impaired HRR, which is not compensated by NHEJ. Given these findings, even if a small number of JCV T-antigen positive cells would survive genotoxic treatment, it could result in a population in which the balance between NHEJ and HRR shifts towards less faithful NHEJ. This might well result in an accumulation of spontaneous mutations and possibly the selection of new cellular adaptations important in tumor initiation and progression.

Although the perennial question whether altered DNA repair could enhance malignant growth in fully formed tumors remains to be answered, findings in this study suggest how viral oncoprotein could contribute to the development of genomic instability during the course of primary tumor growth and recurrences. Because of recent advances, it is now possible to extend these studies to murine central nervous system (CNS) stem cells including partially differentiated neuronal and glial precursors. Defining abnormalities of DNA repair in such a cellular model will support our understanding of CNS tumorigenesis.

Acknowledgements

We gratefully acknowledge Jessica Otte for her technical support. This work was supported by grants from NIH: RO1CA095518-01 (KR) and PO1 NS36466-06 (KK, KR).

References

1. Kleihues P, Louis DN, Scheithauer BW, Rorke LB, Reifenberger G, Burger PC, Cavenee WK. The WHO classification of tumors of the nervous system. J Neuropathol Exp Neurol 2002;61:215–25; discussion 26–9.
2. Longo M, Fiumara F, Pandolfo I, Lavagnini L, Blandino G. [Metastases of the sub-arachnoidal space from medulloblastoma. Computed tomography study]. J Radiol 1982;63:279–81.
3. Bigner SH, Mark J, Friedman HS, Biegel JA, Bigner DD. Structural chromosomal abnormalities in human medulloblastoma. Cancer Genet Cytogenet 1988;30:91–101.
4. Reardon DA, Michalkiewicz E, Boyett JM, Sublett JE, Entrekin RE, Ragsdale ST, Valentine MB, Behm FG, Li H, Heideman RL, Kun LE, Shapiro DN, et al. Extensive genomic abnormalities in childhood medulloblastoma by comparative genomic hybridization. Cancer Res 1997;57:4042–7.
5. Badiali M, Pession A, Basso G, Andreini L, Rigobello L, Galassi E, Giangaspero F. N-myc and c-myc oncogenes amplification in medulloblastomas. Evidence of particularly aggressive behavior of a tumor with c-myc amplification. Tumori 1991;77:118–21.
6. Zurawel RH, Chiappa SA, Allen C, Raffel C. Sporadic medulloblastomas contain oncogenic β-catenin mutations. Cancer Res 1998;58: 896–9.
7. Kozmik Z, Sure U, Ruedi D, Busslinger M, Aguzzi A. Deregulated expression of *PAX5* in medulloblastoma. Proc Natl Acad Sci USA 1995;92:5709–13.
8. Del Valle L, Wang JY, Lassak A, Peruzzi F, Croul S, Khalili K, Reiss K. Insulin-like growth factor I receptor signaling system in JC virus T-antigen induced primitive neuroectodermal tumors–medulloblastomas. J Neurovirol 2002;8 (Suppl. 2):138–47.
9. Patti R, Reddy CD, Geoerger B, Grotzer MA, Raghunath M, Sutton LN, Phillips PC. Autocrine secreted insulin-like growth factor-I stimulates MAP kinase- dependent mitogenic effects in human primitive neuroectodermal tumor/medulloblastoma. Int J Oncol 2000;16:577–84.
10. Reiss K. Insulin-like growth factor-I receptor – a potential therapeutic target in medulloblastomas. Expert Opin Ther Targets 2002;6:539–44.
11. Wang JY, Del Valle L, Gordon J, Rubini M, Romano G, Croul S, Peruzzi F, Khalili K, Reiss K. Activation of the IGF-IR system contributes to malignant growth of human and mouse medulloblastomas. Oncogene 2001;20:3857–68.
12. Del Valle L, Gordon J, Assimakopoulou M, Enam S, Geddes JF, Varakis JN, Katsetos CD, Croul S, Khalili K. Detection of JC virus DNA sequences and expression of the viral regulatory protein T-antigen in tumors of the central nervous system. Cancer Res 2001;61:4287–93.
13. Del Valle L, Gordon J, Enam S, Delbue S, Croul S, Abraham S, Radhakrishnan S, Assimakopoulou M, Katsetos CD, Khalili K. Expression of human neurotropic polyomavirus JCV late gene product agnoprotein in human medulloblastoma. J Natl Cancer Inst 2002;94:267–73.
14. Krynska B, Otte J, Franks R, Khalili K, Croul S. Human ubiquitous JCV(CY) T-antigen gene induces brain tumors in experimental animals. Oncogene 1999;18:39–46.
15. Rollison DE, Utaipat U, Ryschkewitsch C, Hou J, Goldthwaite P, Daniel R, Helzlsouer KJ, Burger PC, Shah KV, Major EO. Investigation of human brain tumors for the presence of polyomavirus genome sequences by two independent laboratories. Int J Cancer 2005;113:769–74.
16. Del Valle L, Gordon J, Ferrante P, Khalili K. JC virus in experimental and clinical brain tumors Human Polyoviruses molecular and clinical perspectives, 1st ed. New York: Wiley-Liss, 2001. 409–30.
17. Krynska B, Del Valle L, Croul S, Gordon J, Katsetos CD, Carbone M, Giordano A, Khalili K. Detection of human neurotropic JC virus DNA sequence and expression of the viral oncogenic protein in pediatric medulloblastomas. Proc Natl Acad Sci USA 1999;96:11519–24.
18. Sullivan CS, Tremblay JD, Fewell SW, Lewis JA, Brodsky JL, Pipas JM. Species-specific elements in the large T-antigen J domain are required for cellular transformation and DNA replication by simian virus 40. Mol Cell Biol 2000;20:5749–57.
19. Khalili K, Stoner GI. Human Polyomaviruses: molecular and clinical perspectives. New York: Wiley-Liss, 2001.
20. Hunter DJ, Gurney EG. The genomic instability associated with integrated simian virus 40 DNA is dependent on the origin of replication and early control region. J Virol 1994;68:787–96.
21. Kappler R, Pietsch T, Weggen S, Wiestler OD, Scherthan H. Chromosomal imbalances and DNA amplifications in SV40 large T-antigen induced primitive neuroectodermal tumor cell lines of the rat. Carcinogenesis 1999;20:1433–8.
22. Ramel S, Sanchez CA, Schimke MK, Neshat K, Cross SM, Raskind WH, Reid BJ. Inactivation of p53 and the development of tetraploidy in the elastase-SV40 T antigen transgenic mouse pancreas. Pancreas 1995;11:213–22.
23. Ricciardiello L, Baglioni M, Giovannini C, Pariali M, Cenacchi G, Ripalti A, Landini MP, Sawa H, Nagashima K, Frisque RJ, Goel A, Boland CR, et al. Induction of chromosomal instability in colonic cells by the human polyomavirus JC virus. Cancer Res 2003;63: 7256–62.
24. Woods C, LeFeuvre C, Stewart N, Bacchetti S. Induction of genomic instability in SV40 transformed human cells: sufficiency of the N-terminal 147 amino acids of large T antigen and role of *pRB* and *p53*. Oncogene 1994;9:2943–50.
25. Hoeijmakers JH. Genome maintenance mechanisms for preventing cancer. Nature 2001;411:366–74.
26. Khanna KK, Jackson SP. DNA double-strand breaks: signaling, repair and the cancer connection. Nat Genet 2001;27:247–54.
27. Castello MA, Clerico A, Deb G, Dominici C, Fidani P, Donfrancesco A. High-dose carboplatin in combination with etoposide (JET regimen) for childhood brain tumors. Am J Pediatr Hematol Oncol 1990; 12:297–300.
28. Chi SN, Gardner SL, Levy AS, Knopp EA, Miller DC, Wisoff JH, Weiner HL, Finlay JL. Feasibility and response to induction chemotherapy intensified with high-dose methotrexate for young children with newly diagnosed high-risk disseminated medulloblastoma. J Clin Oncol 2004;22:4881–7.
29. Sexauer CL, Khan A, Burger PC, Krischer JP, van Eys J, Vats T, Ragab AH. Cisplatin in recurrent pediatric brain tumors. A POG Phase II study. A Pediatric Oncology Group Study. Cancer 1985;56:1497–501.
30. Walker RW, Allen JC. Cisplatin in the treatment of recurrent childhood primary brain tumors. J Clin Oncol 1988;6:62–6.
31. Pierce AJ, Johnson RD, Thompson LH, Jasin M. XRCC3 promotes homology-directed repair of DNA damage in mammalian cells. Genes Dev 1999;13:2633–8.
32. Trojanek J, Ho T, Del Valle L, Nowicki M, Wang JY, Lassak A, Peruzzi F, Khalili K, Skorski T, Reiss K. Role of the insulin-like growth factor I/insulin receptor substrate 1 axis in *Rad51* trafficking and DNA repair by homologous recombination. Mol Cell Biol 2003; 23:7510–24.
33. Schindewolf C, Lobenwein K, Trinczek K, Gomolka M, Soewarto D, Fella C, Pargent W, Singh N, Jung T, Hrabe de Angelis M. Comet assay as a tool to screen for mouse models with inherited radiation sensitivity. Mamm Genome 2000;11:552–4.
34. Ludwig T, Eggenschwiler J, Fisher P, D'Ercole AJ, Davenport ML, Efstratiadis A. Mouse mutants lacking the type 2 IGF receptor (IGF2R) are rescued from perinatal lethality in Igf2 and Igf1r null backgrounds. Dev Biol 1996;177:517–35.
35. Labhart P. Nonhomologous DNA end joining in cell-free systems. Eur J Biochem 1999;265:849–61.
36. Lassak A, Del Valle L, Peruzzi F, Wang JY, Enam S, Croul S, Khalili K, Reiss K. Insulin receptor substrate 1 translocation to the nucleus by the human JC virus T-antigen. J Biol Chem 2002;277:17231–8.
37. Wang JY, Del Valle L, Peruzzi F, Trojanek J, Giordano A, Khalili K, Reiss K. Polyomaviruses and cancer-interplay between viral proteins and signal transduction pathways. J Exp Clin Cancer Res 2004;23:373–83.
38. Krynska B, Del Valle L, Gordon J, Otte J, Croul S, Khalili K. Identification of a novel *p53* mutation in JCV-induced mouse medulloblastoma. Virology 2000;274:65–74.
39. Chipitsyna G, Slonina D, Siddi0qui K, Peruzzi F, Skorski T, Reiss K, Sawaya BE, Khalili K, Amini S. HIV-1 Tat increases cell survival in response to cisplatin by stimulating *Rad51* gene expression. Oncogene 2004;23:2664–71.
40. Del Valle L, Enam 0S, Lara C, Ortiz-Hidalgo C, Katsetos CD, Khalili K. Detection of JC polyomavirus DNA sequences and cellular localization of T-antigen and agnoprotein in oligodendrogliomas. Clin Cancer Res 2002;8:3332–40.

41. Trojanek J, Croul S, Ho T, Wang JY, Darbinyan A, Nowicki M, Valle LD, Skorski T, Khalili K, Reiss K. T-antigen of the human polyomavirus JC attenuates faithful DNA repair by forcing nuclear interaction between IRS-1 and *Rad51*. J Cell Physiol 2006;206:35–46.
42. Paull TT, Rogakou EP, Yamazaki V, Kirchgessner CU, Gellert M, Bonner WM. A critical role for histone H2AX in recruitment of repair factors to nuclear foci after DNA damage. Curr Biol 2000;10:886–95.
43. Bergsagel DJ, Finegold MJ, Butel JS, Kupsky WJ, Garcea RL. DNA sequences similar to those of simian virus 40 in ependymomas and choroid plexus tumors of childhood. N Engl J Med 1992;326:988–93.
44. Khalili K, Del Valle L, Wang JY, Darbinian N, Lassak A, Safak M, Reiss K. T-antigen of human polyomavirus JC cooperates with IGF-IR signaling system in cerebellar tumors of the childhood-medulloblastomas. Anticancer Res 2003;23:2035–41.
45. Testa JR, Carbone M, Hirvonen A, Khalili K, Krynska B, Linnainmaa K, Pooley FD, Rizzo P, Rusch V, Xiao GH. A multi-institutional study confirms the presence and expression of simian virus 40 in human malignant mesotheliomas. Cancer Res 1998;58:4505–9.
46. Okamoto H, Mineta T, Ueda S, Nakahara Y, Shiraishi T, Tamiya T, Tabuchi K. Detection of JC virus DNA sequences in brain tumors in pediatric patients. J Neurosurg 2005;102 (Suppl. 3):294–8.
47. Del Valle L, White MK, Enam S, Oviedo SP, Bromer MQ, Thomas RM, Parkman HP, Khalili K. Detection of JC virus DNA sequences and expression of viral T antigen and agnoprotein in esophageal carcinoma. Cancer 2005;103:516–27.
48. London WT, Houff SA, McKeever PE, Wallen WC, Sever JL, Padgett BL, Walker DL. Viral-induced astrocytomas in squirrel monkeys. Prog Clin Biol Res 1983;105:227–37.
49. Major EO, Mourrain P, Cummins C. JC virus-induced owl monkey glioblastoma cells in culture: biological properties associated with the viral early gene product. Virology 1984;136:359–67.
50. Walker DL, Padgett BL, ZuRhein GM, Albert AE, Marsh RF. Human papovavirus (JC): induction of brain tumors in hamsters. Science 1973;181:674–6.
51. Zu Rhein GM, Varakis J. Perinatal induction of medulloblastomas in Syrian golden hamsterbe a human polyomavirus JC. Natl Cancer Inst Monogr 1979;51:205–08.
52. Ohsumi S, Motoi M, Ogawa K. Induction of undifferentiated tumors by JC virus in the cerebrum of rats. Acta Pathol Jpn 1986;36:815–25.
53. Small JA, Scangos GA, Cork L, Jay G, Khoury G. The early region of human papovavirus JC induces dysmyelination in transgenic mice. Cell 1986;46:13–8.
54. Bollag B, Prins C, Snyder EL, Frisque RJ. Purified JC virus T and T′ proteins differentially interact with the retinoblastoma family of tumor suppressor proteins. Virology 2000;274:165–78.
55. Staib C, Pesch J, Gerwig R, Gerber JK, Brehm U, Stangl A, Grummt F. p53 inhibits JC virus DNA replication in vivo and interacts with JC virus large T-antigen. Virology 1996;219:237–46.
56. Akyuz N, Boehden GS, Susse S, Rimek A, Preuss U, Scheidtmann KH, Wiesmuller L. DNA substrate dependence of p53-mediated regulation of double-strand break repair. Mol Cell Biol 2002;22:6306–17.
57. Bertrand P, Saintigny Y, Lopez BS. *p53*'s double life: transactivation-independent repression of homologous recombination. Trends Genet 2004;20:235–43.
58. Restle A, Janz C, Wiesmuller L. Differences in the association of p53 phosphorylated on serine 15 and key enzymes of homologous recombination. Oncogene 2005;24:4380–7.
59. Fei ZL, D'Ambrosio C, Li S, Surmacz E, Baserga R. Association of insulin receptor substrate 1 with simian virus 40 large T antigen. Mol Cell Biol 1995;15:4232–39.
60. Zhou-Li F, Xu SQ, Dews M, Baserga R. Co-operation of simian virus 40 T antigen and insulin receptor substrate-1 in protection from apoptosis induced by interleukin-3 withdrawal. Oncogene 1997;15: 961–70.
61. Prisco M, Santini F, Baffa R, Liu M, Drakas R, Wu A, Baserga R. Nuclear translocation of insulin receptor substrate-1 by the simian virus 40 T antigen and the activated type 1 insulin-like growth factor receptor. J Biol Chem 2002;277:32078–85.
62. Tu X, Batta P, Innocent N, Prisco M, Casaburi I, Belletti B, Baserga R. Nuclear translocation of insulin receptor substrate-1 by oncogenes and Igf-I. Effect on ribosomal RNA synthesis. J Biol Chem 2002;277: 44357–65.
63. Drakas R, Tu X, Baserga R. Control of cell size through phosphorylation of upstream binding factor 1 by nuclear phosphatidyl inositol 3-kinase. Proc Natl Acad Sci USA 2004;101:9272–6.
64. Wu A, Tu X, Prisco M, Baserga R. Regulation of upstream binding factor 1 activity by insulin-like growth factor I receptor signaling. J Biol Chem 2005;280:2863–72.